

RESEARCH

Open Access



# Removal of Brilliant Blue R and Victoria Blue R dyes from textile wastewater by adsorption method using pomegranate peel

Bediha Akmese<sup>1\*</sup>

## Abstract

This study investigated the removal of Brilliant Blue R (BBR) and Victoria Blue R (VBR), commonly used dyes in the textile industry, from wastewater using the pomegranate peel with an adsorption method. Pomegranate peel was characterized by using X-ray diffraction (XRD), Brunauer, Emmet ve Teller (BET), scanning electron microscopy (SEM), Fourier transform infrared spectrophotometer (FT-IR), thermogravimetric analysis (TGA), and zeta potential. For both dyes, pH, adsorbent amount, contact time, salt effect, and wastewater parameters were investigated in the batch system, while adsorbent amount and flow rate parameters were investigated in the continuous system. The adsorption results of both dyes on pomegranate peel indicate that they fit the pseudo-second-order kinetic model. The adsorption isotherms of both dyes were found to be compatible with the Langmuir isotherm model. In the thermodynamic study, it was determined that the adsorption process was spontaneous ( $\Delta G^\circ < 0$ ) and exothermic ( $\Delta H^\circ < 0$ ). It was decided that pomegranate peel is a suitable adsorbent for the adsorption of BBR and VBR dyes. Finally, the adsorption yields for removing BBR and VBR from wastewater using pomegranate peel were 90.38% and 100%, respectively. This result shows that the high adsorption efficiency obtained for both dyes makes it possible for pomegranate peel to be widely applied as an adsorbent in wastewater treatment.

**Keywords** Brilliant Blue R, Victoria Blue R, Pomegranate peel, Wastewater, Adsorption

## Introduction

BBR is a synthetic anionic dye commonly used in the textile industry and biochemistry laboratories for dyeing and evaluating proteins [1–2]. BBR's non-degradable structure poses a danger to the environment and human health [3]. VBR is a cationic triphenylmethane dye widely used in the textile, leather, food, cosmetics, and pharmaceutical sectors. VBR can be mutagenic and carcinogenic to humans and aquatic organisms [4, 5]. Dyes mixed into

waterways as a result of rapidly increasing industrial activities can have harmful effects, even at low concentrations, due to their toxic and complex structures. While posing a threat to human health, they also disrupt the aesthetic and biological balance in the aquatic ecosystem [6].

Different physical and chemical techniques have been employed to eliminate dyes from wastewater [3]. Among these, adsorption stands out as a proven and effective method for dye removal [7]. This technology is appealing due to its low processing costs, straightforward process flow, and user-friendliness [8]. Adsorption effectively targets non-biodegradable pollutants in water [9]. In adsorption methods, the quantity of substance captured by the adsorbent is influenced by the nature of the

\*Correspondence:

Bediha Akmese  
bedihaakmese@hitit.edu.tr

<sup>1</sup>Vocational School of Health Services, Department of Pharmacy Services, Hitit University, Corum, Turkey



© The Author(s) 2025. **Open Access** This article is licensed under a Creative Commons Attribution-NonCommercial-NoDerivatives 4.0 International License, which permits any non-commercial use, sharing, distribution and reproduction in any medium or format, as long as you give appropriate credit to the original author(s) and the source, provide a link to the Creative Commons licence, and indicate if you modified the licensed material. You do not have permission under this licence to share adapted material derived from this article or parts of it. The images or other third party material in this article are included in the article's Creative Commons licence, unless indicated otherwise in a credit line to the material. If material is not included in the article's Creative Commons licence and your intended use is not permitted by statutory regulation or exceeds the permitted use, you will need to obtain permission directly from the copyright holder. To view a copy of this licence, visit <http://creativecommons.org/licenses/by-nc-nd/4.0/>.

adsorbent and the substance itself and by physicochemical factors, including concentration, temperature, adsorbent quantity, and solution pH [10].

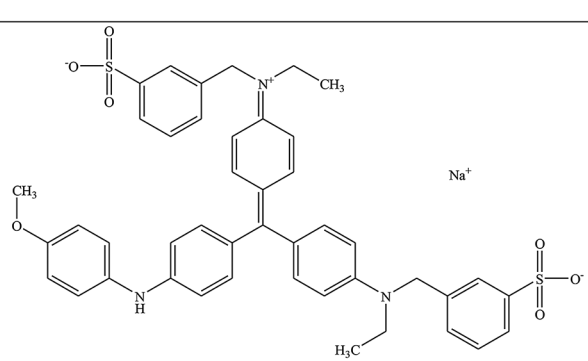
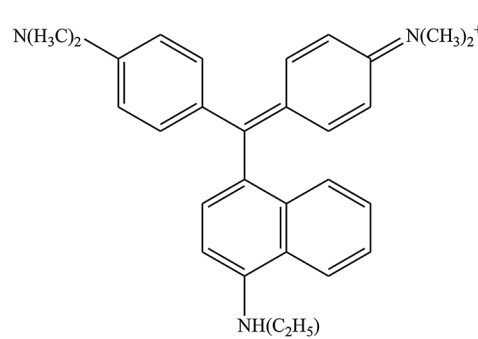
In previous studies on the removal of BBR by the adsorption method, a porous nanocrystalline cobalt ferrite composite [11], nigella sativa [1],  $\alpha$ -chitin nanoparticles [12], corncob [13], wheat bran [14], apricot stone [15] and coconut pulp [16] were used as adsorbents. In the adsorption methods used to remove VBR from wastewater, calcined eggshell [17], chitosan-immobilized bone meal [18], magnetic microparticles bearing the double salt of Fe(II) and Co(II) [19], and chestnut tannins [20] were used. In recent years, various bio-based and low-cost adsorbents, including agricultural and animal wastes, have been effectively applied in the removal of dyes and antibiotics from wastewater [21]. No study was found in the literature that examined the kinetic, isotherm, and thermodynamic parameters in detail for the deposition of BBR and VBR dyes with pomegranate peel.

Pomegranate peels are byproducts of the food industry. Pomegranate juice produces waste, primarily consisting of pomegranate peels (approximately 78%) [22]. Disposing of these wastes incurs costs, underscoring the need for alternative solutions [23]. Using agricultural byproducts as adsorbents has garnered significant attention due

to their low cost, abundant availability, high fixed carbon content, and porous structure [24]. The use of pomegranate peel, which contains compounds such as tannins, phenolic acids, and flavonoids with antioxidant, anti-inflammatory, anticancer, and antimicrobial properties, as an adsorbent for treating wastewater contaminants shows promise for sustainable, environmentally friendly technologies [25–26].

In this study, the effectiveness of pomegranate peel in removing BBR and VBR dyes used in the textile industry, whose chemical formulas are listed in Table 1, was evaluated using the adsorption method. For the removal of dyes, time, pH, adsorbent amount, contact time, and salt effect were investigated in the batch system, and adsorbent amount and flow rate parameters were investigated in the continuous system. The adsorption potential of pomegranate peel was also examined using the results of kinetics, equilibrium isotherms, and thermodynamic experiments. Pomegranate peel was characterized by XRD, BET surface area, SEM, FT-IR, TGA, and zeta potential and successfully applied to remove dyes from wastewater.

**Table 1** Chemical structure of the dyes

Dye	Chemical Structure of Dyes	Molecular Formula	Molecular Weight (g/mol)
BBR		$C_{45}H_{44}N_3NaO_7S_2$	825.97
VBR		$C_{29}H_{32}N_3Cl$	458.05

## Materials and methods

### Chemicals

BBR, VBR, and sodium chloride were purchased from Sigma-Aldrich. Riedel de Haen provided sodium hydroxide and 37% hydrochloric acid (d:1.19 g/mL). Pure water was used throughout all experiments.

### Apparatus

The concentrations of the BBR and VBR dyes were measured using an ultraviolet (UV)/visible region spectrophotometer (Thermo Genesys 10 S brand). The maximum wavelengths of BBR and VBR were determined as 586 and 615 nm, respectively. The calibration graph for BBR was drawn in the concentration range of 0.5–50 mg/L. The linearity of the graph was found to be  $R^2 = 0.9993$  and its equation was  $y = 0.0263x$ . The calibration graph for VBR was drawn in the concentration range of 0.5–50 mg/L. The linearity of the graph was found to be  $R^2 = 0.9973$  and its equation was  $y = 0.134x$ . Human Corp., Zeneer Power I brand, was used as a pure water device. Peristaltic pump (Ismatec, Wertheim, Germany) was used to determine the flow in the continuous system.

### Working standard solutions

By dissolving the BBR and VBR in distilled water, a stock solution of 200 mg/L BBR and VBR was created. Dye solutions with different concentrations were taken from the stock solution and diluted with pure water. To adjust the pH of the dye solutions, 0.1 mol/L HCl, 1.0 mol/L HCl, 0.1 mol/L NaOH, and 1.0 mol/L NaOH solutions were prepared using distilled water as the solvent. The solutions were made daily and kept in the freezer at +4 °C.

### Preparation of adsorbents

The pomegranate used in the study was purchased from the market in Corum, Turkey. After being separated and cleaned with distilled water, the pomegranate peel was dried until it lost weight at 50 °C. After drying, pomegranate peels were crushed and sieved using a 150 µm screen.

### Characterization of pomegranate Peel

XRD analyses were done with an X-ray diffractometer (Rigaku SmartLab) in the reading range of 3–90° (2θ). The average pore radius and total pore volume were determined using the BET (Quantachrome/IQ-Chemi) device. The surface morphology of pomegranate peel was examined using SEM (JSM-5600). The chemical structure analysis of pomegranate peel was performed using an FT-IR spectrometer (Thermo Nicolet iS10 FTIR Spectrometer). Thermogravimetric analysis (TGA) measurement was obtained using a simultaneous differential thermal analyzer (SDTQ600). Detection of particle size

measurements of pomegranate peel was conducted using a particle size and zeta potential measurement device in nanoparticles (Zetasizer/Nano ZSP).

### Adsorption studies

This study found optimum adsorption conditions for the adsorption of BBR and VBR dyes with pomegranate peel in batch and continuous systems. The batch system's parameters were studied, including the pH, amount of adsorbent, contact time, and salt effect. The adsorbent amount and flow rate parameters were studied in the continuous system.

The percent of dye removed from the solution was calculated using the formula below [27]:

$$\%_{removal} = \frac{C_0 - C_i}{C_0} \quad (1)$$

where  $C_0$  (mg/L) is the dye concentration before adsorption,  $C_i$  (mg/L) is the dye concentration after adsorption.

The following formula was used to determine the adsorption capacity after equilibrium [28]:

$$q_e = (C_0 - C_e) \frac{V}{m} \quad (2)$$

where  $q_e$  (mg/g) is adsorption capacity,  $C_0$  (mg/L) is the dye concentration before adsorption,  $C_e$  (mg/L) is the dye concentration at equilibrium,  $V$  (L) is the dye solution volume and  $m$  (g) is the adsorbent amount (g).

### Adsorption kinetics

In investigating the adsorption mechanism, the pseudo-first-order kinetic model in Eq. (3) [29], the pseudo-second-order kinetic model in Eq. (4) [30], and the intra-particle diffusion kinetic model in Eq. (5) [31] were used. The most suitable adsorption mechanism was compared.

$$\ln(q_e - q_t) = \ln q_e - K_{s1}t \quad (3)$$

$$\frac{t}{q_t} = \frac{1}{K_{s2}q_e^2} + \frac{1}{q_e}t \quad (4)$$

$$q_t = K_p t^{0.5} + C \quad (5)$$

where  $q_e$  (mg/g) is adsorption capacity (mg/g),  $q_t$  (mg/g) is adsorption capacity at any given time,  $t$  (min) is time,  $K_{s1}$  (1/min) is the pseudo-first-order rate constant,  $K_{s2}$  (g/mg min) is the pseudo-first-order rate constant,  $K_p$  (mg/g min<sup>2</sup>) is the intraparticle diffusion constant and  $C$  (mg/g) is a constant that indicates the adsorption process layer thickness.

### Adsorption isotherms

The adsorption isotherm describes the equilibrium distribution between two phases. In an attempt to correlate with the experimental results, the Freundlich isotherm model in Eq. (6) [32], the Langmuir isotherm model in Eq. (7) [33], and the D-R isotherm model in Eq. (8) [34] were used.

$$\ln q_e = \ln K_F + \frac{1}{n} \ln C_e \quad (6)$$

$$\frac{1}{q_e} = \frac{1}{q_{max}} + \left[ \frac{1}{q_{max} K_L} \right] \frac{1}{C_e} \quad (7)$$

$$\ln q_e = \ln q_{max} - \beta \epsilon^2 \quad (8)$$

$\epsilon$  is defined as:

$$\epsilon = RT \ln \left[ 1 + \frac{1}{C_e} \right] \quad (9)$$

where  $q_e$  (mol/g) is the adsorption capacity, and  $q_{max}$  (mol/g) is the maximum adsorption capacity,  $C_e$  (mol/L) is the dye concentration at equilibrium,  $K_F$  (L/g) is the Freundlich isotherm constant,  $K_L$  (L/mol) is the Langmuir isotherm constants,  $\beta$  (mol<sup>2</sup>/kJ<sup>2</sup>) is the constants related to adsorption energy,  $\epsilon$  (kJ/mol) is the adsorption potential,  $T$  (K) is the absolute temperature and  $R$  (8.314 J/mol K) is gas constant.

To minimize the error distribution between the calculated theoretical model correlations and the experimental data, the Chi-square statistic ( $\chi^2$ ), the hybrid fractional error (HYBRID), and the sum of the absolute errors (EABS) functions were employed to identify the kinetic and isotherm models that best matched the data [35–36].

$$\chi^2 = \sum_{i=1}^n \frac{(q_{e,exp} - q_{e,cal})^2}{q_{e,cal}} \quad (10)$$

$$HYBRID = \sum_{i=1}^n \left[ \frac{(q_{e,exp} - q_{e,cal})^2}{q_{e,exp}} \right]_i \quad (11)$$

$$EABS = \sum_{i=1}^n |q_{e,exp} - q_{e,cal}|_i \quad (12)$$

where  $q_{e,exp}$  is experimental adsorption capacity,  $q_{e,cal}$  is calculated adsorption capacity, and  $n$  is study data.

### Thermodynamic parameters

By examining the effect of temperature on adsorption processes, it can be understood whether the process takes heat (endothermic) or gives heat (exothermic) and the most efficient temperature conditions can be

determined accordingly [27]. Thermodynamic parameters reveal whether adsorption occurs spontaneously and the interaction strength between the adsorbent and the adsorbate [28]. Three parameters, enthalpy change ( $\Delta H^\circ$ ), Gibbs free energy ( $\Delta G^\circ$ ) and entropy change ( $\Delta S^\circ$ ) were studied to evaluate the thermodynamic properties of the adsorption process. Thermodynamic parameters were calculated with the following equations [37]:

$$\Delta G^\circ = -RT \ln K_L \quad (13)$$

$$\ln K_L = -\frac{\Delta H^\circ}{RT} + \frac{\Delta S^\circ}{R} \quad (14)$$

where  $\Delta G^\circ$  (kJ/mol) is Gibbs free energy,  $R$  (8.314 J/mol K) is gas constant,  $T$  (K) is temperature,  $K_L$  (L/mol) is the Langmuir isotherm constants,  $\Delta H^\circ$  (kJ/mol) is the enthalpy change and  $\Delta S^\circ$  (kJ/mol K) is the entropy change.

### Wastewater

The natural wastewater was collected from the wastewater of factories in the Corum-organized industrial zone. It is a mixture of chemical and metallic waste materials from various factories operating in various types of production, including paper, fertilizer, textiles, and metal [38]. Combining dye with wastewater created a 25 mg/L dye solution. Adsorption conditions were chosen as the predetermined optimum conditions.

## Results and discussion

### Characterization of the adsorbent

The study's pomegranate peel was characterized using XRD, BET, SEM, FT-IR, TGA, and zeta potential analysis.

### XRD analysis

In Fig. 1(a), broad and low-intensity peaks were observed at 18.06°, 22.08° and 38.68° in the XRD pattern of pomegranate peel. This shows that the pomegranate peel's crystal structure was less, and there are mostly irregular amorphous regions. In Fig. 1(b), sharp and distinct peaks were observed at 21.84° and 38.65° in the XRD pattern of BBR's adsorption with pomegranate peel. This change in the peaks means that BBR changes the surface properties of the pomegranate peel after adsorption and gives it a more regular structure [39]. In Fig. 1(c), distinct and sharp peaks were observed at 22.18° and 38.66° in the XRD pattern of VBR adsorption with pomegranate peel. The sharp peaks observed after VBR's adsorption with pomegranate peel show that VBR binds to the pomegranate peel during the adsorption process and forms a regular structure on the surface. Consequently, it was concluded that while the pomegranate peel exhibited an amorphous nature before adsorption, the presence of

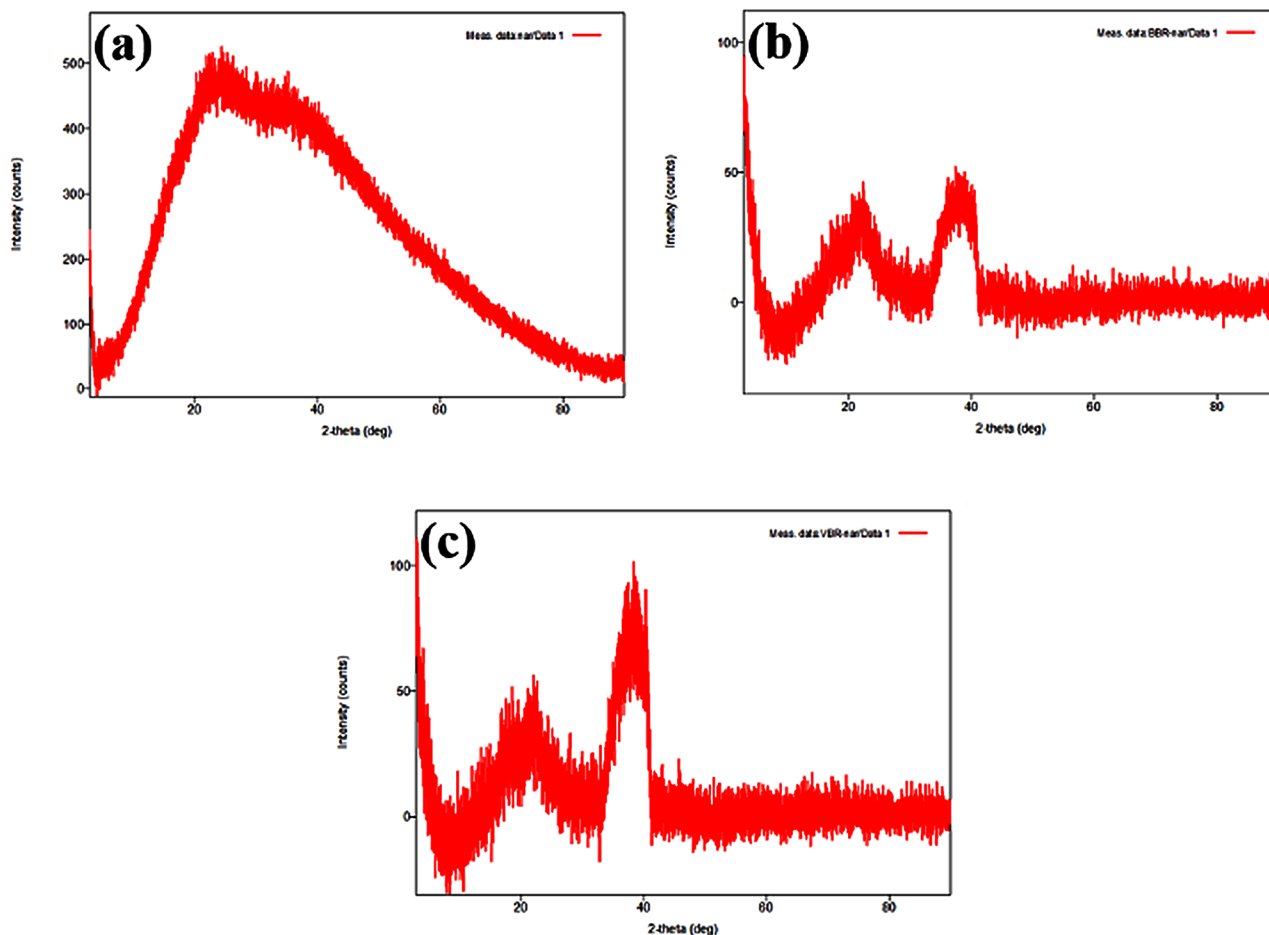


**Fig. 1** XRD patterns of (a) pomegranate peel, (b) BBR after adsorption with pomegranate peel, (c) VBR after adsorption with pomegranate peel

more regular structures increased after adsorption with BBR and VBR, indicating that the adsorption process led to a significant structural transformation in the pomegranate peel [40].

The crystallinity index is a measure that expresses the volumetric ratio of crystalline phase and the percentage of crystalline material in a sample and is also directly related to the average size, structural regularity, and perfection of crystals [41]. The formula used in the calculation of crystallinity index (CrI) is [42]:

$$CrI\% = \frac{I_t - I_a}{I_t} \quad (12)$$

where  $I_t$  is the total intensity and  $I_a$  is the amorphous intensity. Accordingly, in the calculation made based on XRD analysis, the crystallinity index of the pomegranate peel before adsorption was 102.15%, and the crystallinity index of the pomegranate peel after adsorption with BBR and VBR was 124.91% and 127.87%, respectively. The increase in crystallinity observed for both dyes is attributed to the interactions between the dye molecules

**Table 2** BET analysis results of pomegranate peel

BET surface area (m <sup>2</sup> /g)	4.414
Average pore radius (Å)	1306.69
Total pore volume (cc/g)	6.118 10 <sup>-1</sup>

and the adsorbent matrix, resulting in the formation of a more regular structure at the molecular level [43].

#### BET analysis

The calculated BET surface area was 4.414 m<sup>2</sup>/g, the measured pore radius was 1306.69 Å, and the total pore was 6.118 10<sup>-1</sup> cc/g. The BET surface area of 4.414 m<sup>2</sup>/g indicated a large surface area (Table 2). A high surface area means the material can have a high adsorption capacity. In other words, this material can adsorb more substances on its surface. The pore radius of 1306.69 Å indicates that the pomegranate peel has large pores. This shows that the pomegranate peel has a macroporous (large porous) structure [44]. Large porous materials allow gases or liquids to enter and exit more easily. The total pore amount indicated that the pomegranate peel can hold 6.118 10<sup>-1</sup>

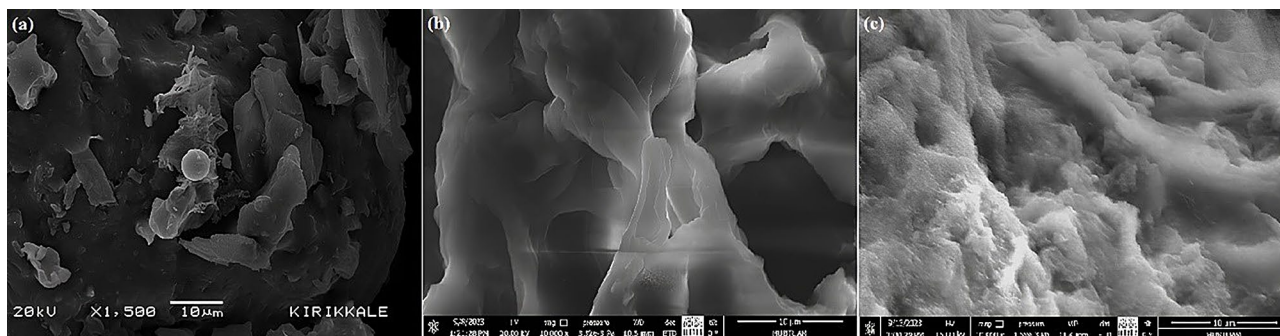


**Fig. 2** SEM pictogram of (a) pomegranate peel, (b) BBR-loaded pomegranate peel and (c) VBR-loaded pomegranate peel

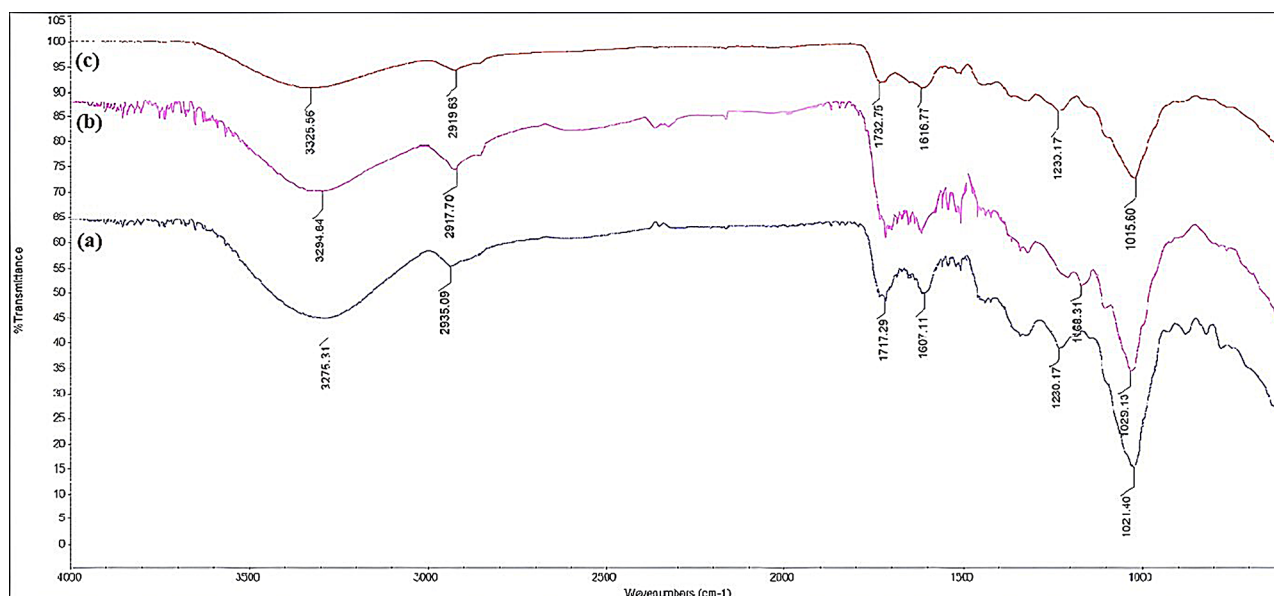


**Fig. 3** FT-IR spectrum of pomegranate peel (a) before adsorption, (b) after adsorption with BBR, and (c) after adsorption with VBR

cc/g volume in its pores. This supports the porous structure and adsorption capacity of the material.

#### SEM analysis

The pomegranate peel used in this study was analyzed with an SEM to examine its morphology. The SEM image of the fracture surface of the unloaded adsorbent is shown in Fig. 2(a), revealing the porous structure of the adsorbent. There are some gaps on the outer surface of the adsorbent that can receive dye molecules. Figures 2(b) and 2(c) belong to BBR and VBR, respectively, adsorbed on the surface of pomegranate peel. The differences in the pomegranate peel's initial surface morphology and the dye's surface morphology after adsorption confirm the presence of dye molecules on the adsorbent. SEM analysis shows that pomegranate peel has a porous and rough surface. This rough structure enables liquids to be more evenly distributed on the surface, thereby increasing the adsorption capacity [45]. These results

support the effectiveness of using pomegranate peel as an adsorbent.

#### FT-IR analysis

The functional groups of the adsorbent involved in the dye removal process can be better understood using FT-IR spectrum analysis, as is well known. The FT-IR spectra of pomegranate peel and BBR and VBR following adsorption with pomegranate peel were compared, and the results are shown in Fig. 3. The FT-IR spectrum of the adsorbent (Fig. 3a) before decolorization exhibited a broad absorption band centered at  $3275\text{ cm}^{-1}$ , corresponding to its O-H stretching vibration of the adsorbent. It corresponds to a C-H stretch of around  $2935\text{ cm}^{-1}$ . It may correspond to a C=O stretch at around  $1717\text{ cm}^{-1}$  and a C-O stretch  $1230\text{ cm}^{-1}$ . The peak around  $1021\text{ cm}^{-1}$  may give the CH<sub>2</sub>-O group. After the adsorption of BBR (Fig. 3b), the bands at 3275, 2935, 1230, and  $1021\text{ cm}^{-1}$  on the immobilized adsorbent shifted to 3294, 2917, 1168, and  $1029\text{ cm}^{-1}$ , respectively, and the bands at

1717 and 1607  $\text{cm}^{-1}$  disappeared. The shift to 3294  $\text{cm}^{-1}$  indicated that BBR may have interacted with the O-H groups on the surface. 1717 and 1607  $\text{cm}^{-1}$  bands may indicate that carbonyl groups interacted with BBR during adsorption. After the adsorption of VBR (Fig. 3c), 3275, 2935, 1717, 1607, and 1021  $\text{cm}^{-1}$  bands on the immobilized adsorbent shifted to 3325, 2919, 1732, 1616, and 1015  $\text{cm}^{-1}$ , respectively. 3325  $\text{cm}^{-1}$  shift indicates that VBR interacts with O-H groups after adsorption. 1732, 1616  $\text{cm}^{-1}$  shift may indicate that VBR interacts with carbonyl groups on the surface. These results indicated that the functional groups on the surface of the pomegranate peel interact with BBR and VBR after adsorption, resulting in stable adsorption on the surface of the adsorbent. This showed that no organic compound is dissolved in the solution and that there is no leakage from the surface of the pomegranate peel.

#### TGA analysis

The thermal behavior of the pomegranate peel occurred in a nitrogen atmosphere at a heating rate of 10  $^{\circ}\text{C}/\text{min}$  and between 30 and 490  $^{\circ}\text{C}$ . Figure 4 shows the TGA curves of pomegranate peel. Accordingly, the sample's thermal weight loss is 14% mass loss in the 30–171.55  $^{\circ}\text{C}$  temperature range. The mass loss observed in this temperature range was due to the evaporation of the

pomegranate peel. Pomegranate peel lost 39% of its mass at 294.25  $^{\circ}\text{C}$ . In this temperature range, cellulose, hemicellulose, and phenolic compounds found in pomegranate peel may begin to decompose. The mass loss of pomegranate peel continues in the temperature range of 350–490  $^{\circ}\text{C}$ , but a less steep decline is observed. This suggests that the thermal degradation of the more resistant components of the pomegranate peel, such as lignin [46], was a contributing factor. At around 500  $^{\circ}\text{C}$ , the pomegranate peel lost approximately 62% of its mass. According to these results, the pomegranate peel is thermally stable up to 171.55  $^{\circ}\text{C}$ .

#### Zeta potential

The zeta potential value of pomegranate peel was  $-18.4$  mV ( $\pm 8.73$  mV). The zeta potential value of BBR after adsorption with pomegranate peel was found to be  $-19.5$  ( $\pm 59.5$  mV), and the zeta potential value of VBR after adsorption with pomegranate peel was found to be  $-14.1$  mV ( $\pm 90.2$  mV). The zeta potential value of the pomegranate peel after adsorption with BBR showed a slight decrease. This indicates that the negative charge on the surface increased after adsorption, and BBR bound to the surface, affecting the surface charge. The zeta potential value of pomegranate peel increased after adsorption with VBR. This change indicates that VBR binds to the

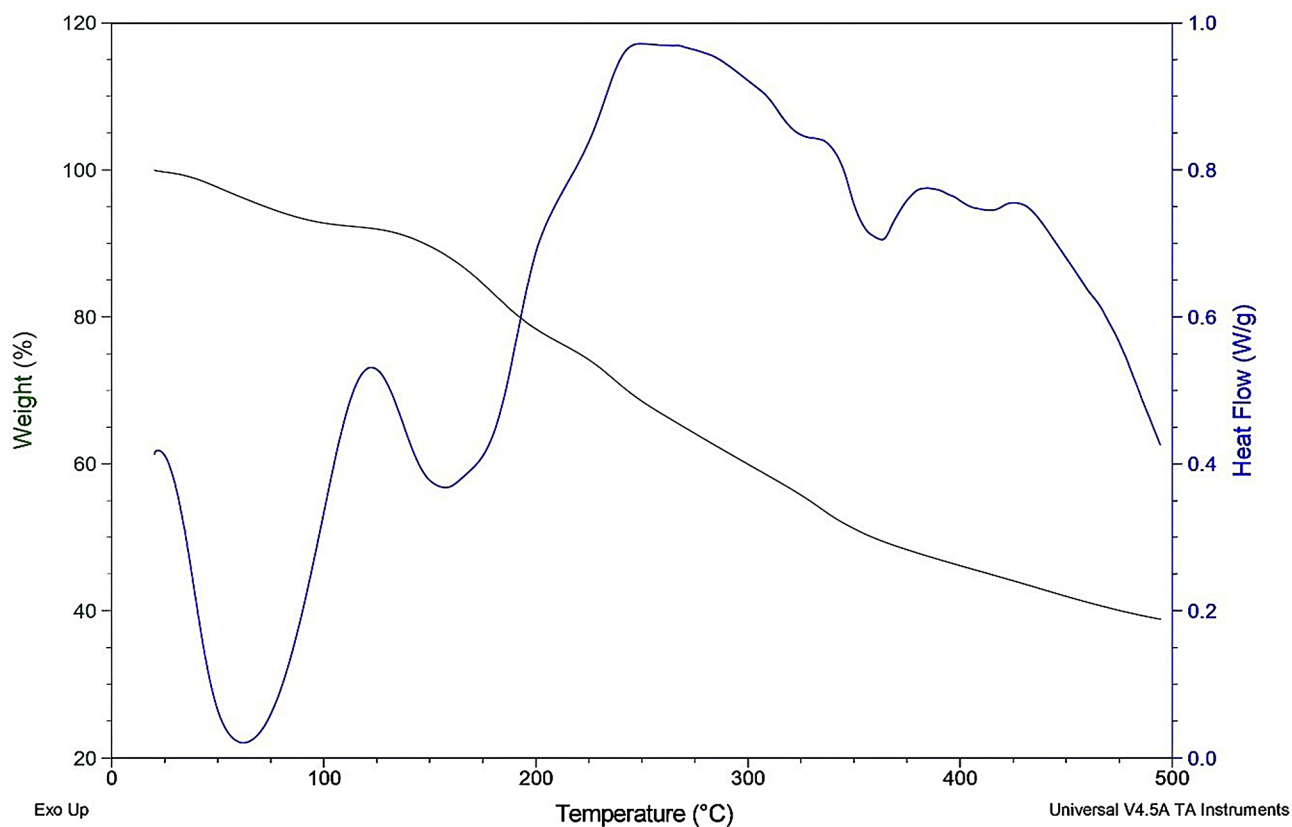
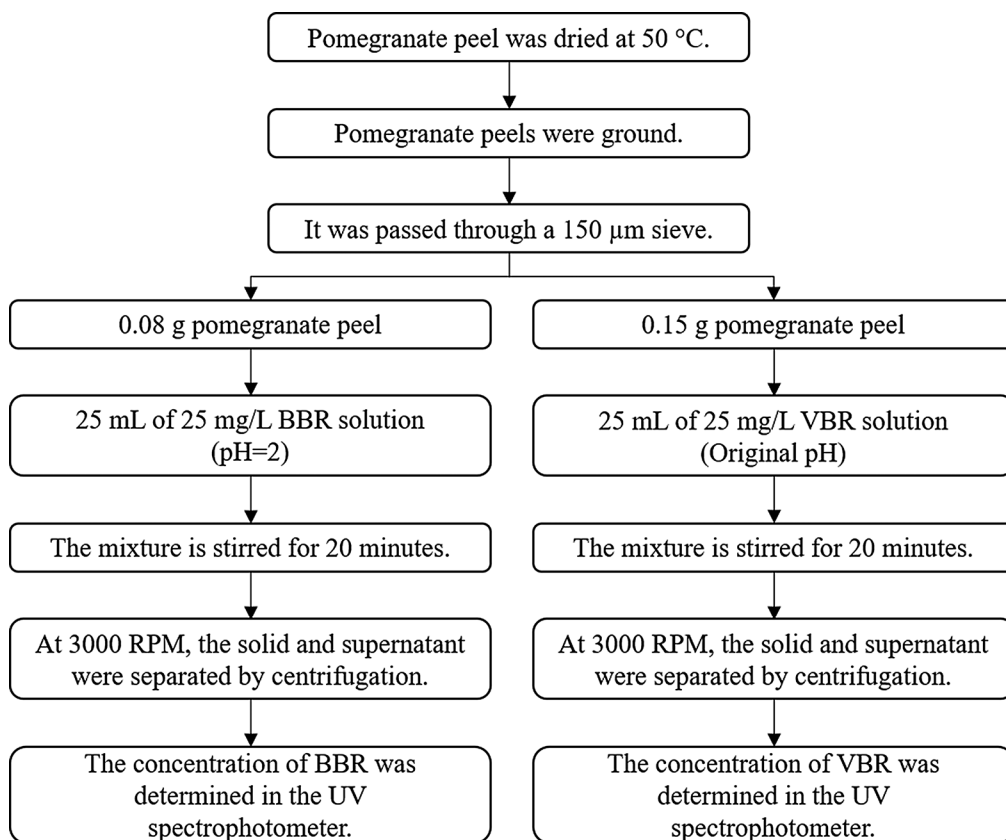


**Fig. 4** Thermogravimetric curve of pomegranate peel



**Scheme. 1** Experimental flow chart of the adsorption of BBR and VBR with pomegranate peel

surface of the pomegranate peel and partially neutralizes the negative charge density on the surface [47].

According to zetasizer results, the particle size of pomegranate peel was 5.526  $\mu\text{m}$ , and the polydispersity index was 0.7960. This value showed that pomegranate peel particles tend to form large clusters in solution. This indicates low stability and needs better surface charge or chemical modification stabilization. After the adsorption of BBR with pomegranate peel, the particle size was 5.653  $\mu\text{m}$ , and the polydispersity index was 1.000. This can be explained by the accumulation of BBR molecules on the surface of the pomegranate peel during the adsorption process, along with a slight increase in particle size. The increase in the polydispersity index suggests that the particles were heterogeneous and that stability issues may arise. After the adsorption of VBR with pomegranate peel, the particle size was 4.051  $\mu\text{m}$ , and the polydispersity index was 0.215. It was observed that the particle sizes became more homogeneous after adsorption; however, a surface structure was formed in which both large and small particles coexisted [42].

#### Adsorption studies in batch system

The optimal conditions for adsorbing pomegranate peel and dyestuffs in a batch system were identified by

considering pH, the amount of adsorbent, contact time, the concentrations of BBR and VBR, and the impact of salt.

#### Effect of pH

In the pH = 2–10 range, the impact of pH on the adsorption of BBR and VBR with pomegranate peel was examined. 25 mg/L dye solutions were prepared. 0.1 mol/L HCl and 0.1 mol/L NaOH solutions were used to adjust the pH of the dye solutions. It was taken from the pH-adjusted dye solutions in 25 mL volume and contacted with 0.1 g of adsorbent for 60 min. At 3000 RPM, the solid and supernatant were separated by centrifugation. Then, the quantitative determination of the supernatant and dye solutions was carried out using a UV spectrophotometer at the maximum wavelength ( $\lambda_{\text{max}} = 586 \text{ nm}$  for BBR and  $\lambda_{\text{max}} = 615 \text{ nm}$  for VBR).

As shown in Fig. 5(a), the maximum adsorption capacity of BBR dye was reached at pH 2. After pH 2, it was observed that the adsorption capacity decreased. The surface of the adsorbent becomes positively charged at acidic pH levels. The adsorbent surface, surrounded by positive ions, and the BBR dyestuff, loaded with negative ions, interact electrostatically. As the pH increases, the adsorption capacity decreases due to the increase of

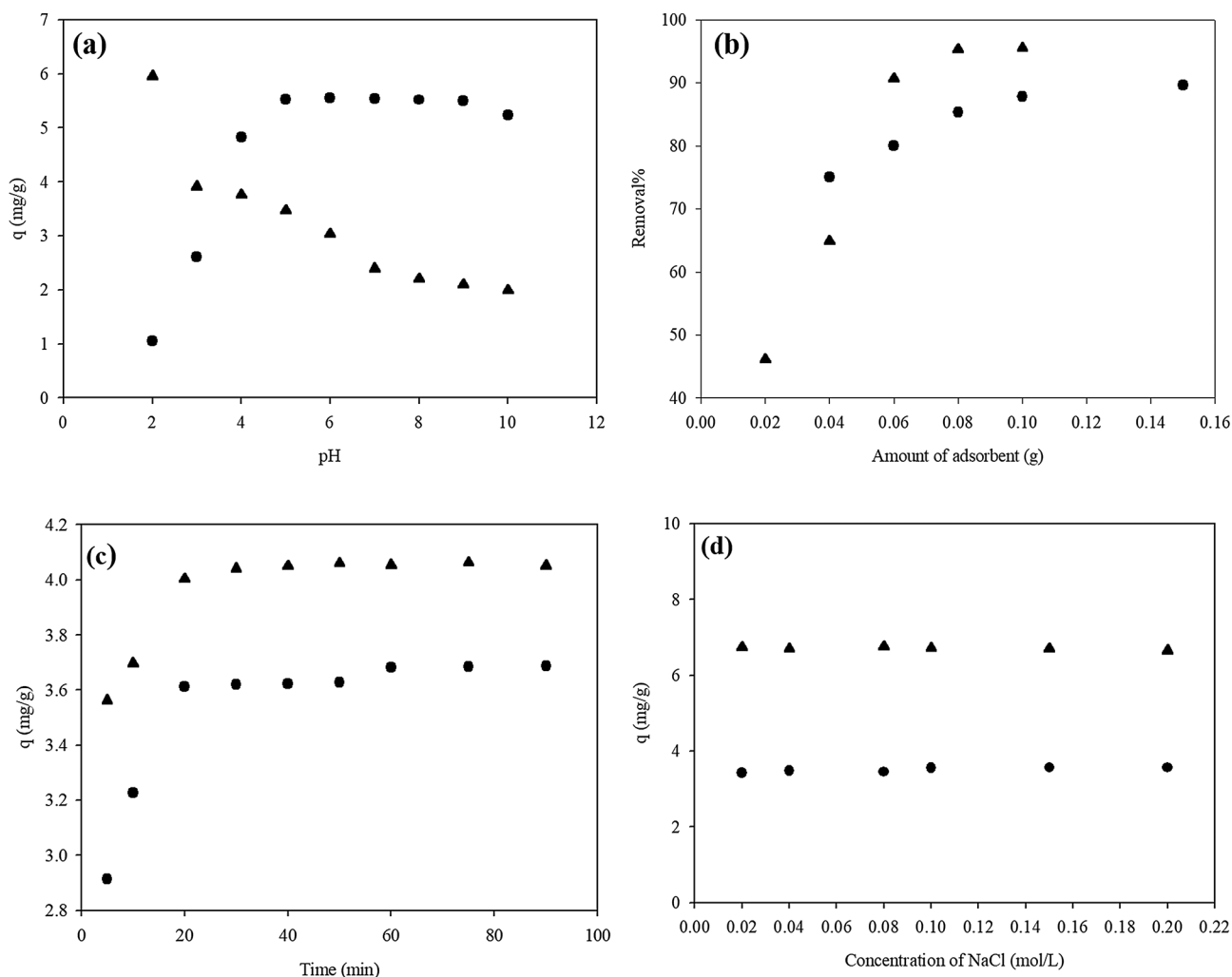


**Fig. 5** Effect of pH (a), adsorbent amount (b), contact time (c) and salt (d) on the adsorption of BBR (▲) and VBR(●) with pomegranate peel

$\text{OH}^-$  ions around the pomegranate peel. According to the results, the optimum pH was determined to be 2. When the pH of the VBR solution was altered between 2 and 5, it is observed that the adsorption capacity increases and then remains nearly constant. The original pH of the dye solution was found to be 6.8. Therefore, the original pH (pH 6.8) of the VBR solution was determined as the optimum pH. Having three amine groups, VBR was positively ionized in a strongly acidic environment. At acidic pH values, the adsorption capacity was low due to competition between VBR ions and  $\text{H}_3\text{O}^+$  ions. At a basic pH, since the surface of the adsorbent was surrounded by negative charges, the electrostatic attraction force between the adsorbent and the dye solution increases. Thus, the capacity was observed to increase.

#### Effect of adsorbent amount

The effects of the adsorbent amount were investigated in the range of 0.02–0.10 g and 0.04–0.15 g for BBR (pH 2) and VBR (original pH), respectively. For this purpose,

25 mL of 25 mg/L dye solutions were taken from each of the two dyes. The adsorption studies were conducted for 60 min at a mixing speed of 250 RPM at the optimum pH of the dye solutions. After adsorption, the liquid and solid components were separated, and the concentrations of each component were quantified using a UV spectrophotometer. Figure 5(b) shows that for both dyes, the adsorption capacity rises as the amount of adsorbent increases. This condition can be explained by adsorption increasing with surface area and staying constant at saturation. The optimum adsorbent amounts were determined to be 0.08 g and 0.15 g for BBR and VBR, respectively.

#### Effect of contact time

The contact time study of adsorption was conducted in the range of 5 to 90 min by adding 0.08 g and 0.15 g of pomegranate peel to of BBR (pH 2) and VBR (original pH) solutions, respectively. For this purpose, 25 mL of 25 mg/L dye solutions were taken from each of the two dyes. It was observed that the adsorption equilibrium

was established within a short time, such as 20 min, for both dyes. Figure 5(c) illustrates the impact of contact time on the adsorption of BBR and VBR onto pomegranate peel. The adsorption processes of BBR and VBR with pomegranate peel are presented in Scheme 1.

### Effect of salt

Wastewater usually contains high concentrations of salt, depending on its source. To investigate how other ions affect the adsorption efficiency in a natural wastewater environment, BBR and VBR solutions containing NaCl at concentrations ranging from 0.02 to 0.20 mol/L were prepared. The adsorption conditions of BBR are as follows: concentration, 25 ppm; solution volume, 25 mL; adsorbent amount, 0.08 g; pH, 2; temperature, 25 °C; and contact time, 20 min. 25 mL, 25 mg/L VBR adsorbent amount: 0.15 g, original pH, contact time: 20 min. The adsorption conditions of BBR were concentration 25 mg/L, solution volume 25 mL, 0.08 g adsorbent amount, pH 2; T 25 °C; contact time 20 min. The adsorption conditions of VBR were concentration 25 mg/L, solution volume 25 mL, 0.15 g adsorbent amount, original pH; T 25 °C; contact time 20 min. BBR and VBR concentrations were determined using a UV spectrophotometer. Figure 5(d) illustrates the impact of NaCl salt on the adsorption of BBR and VBR using pomegranate peel. It was shown that neither dye was considerably impacted by the salt effect when NaCl salt was present.

**Table 3** Kinetic parameters for adsorption of BBR and VBR with pomegranate Peel

	BBR	VBR
Pseudo-first-order kinetic model		
R <sup>2</sup>	0.9215	0.6870
χ <sup>2</sup>	0.0193	0.1321
HYBRID	0.0202	0.1453
EABS	0.4893	1.470
K <sub>s1</sub> (1/min)	0.05113	0.05664
q <sub>e</sub> (mg/g)	0.6400	0.5590
Pseudo-second-order kinetic model		
R <sup>2</sup>	0.9998	0.9999
χ <sup>2</sup>	0.007610	0.004691
HYBRID	0.007678	0.004629
EABS	0.4212	0.2713
K <sub>s2</sub> (g/mg min)	0.1518	0.2118
q <sub>e</sub> (mg/g)	4.270	3.744
Intraparticle diffusion model		
R <sup>2</sup>	0.8765	0.6884
χ <sup>2</sup>	0.01299	0.05339
HYBRID	0.01293	0.05407
EABS	0.5390	1.0001
K <sub>p</sub> (mg/g min <sup>2</sup> )	0.08608	0.09066
C (mg/g)	3.480	2.969

### Adsorption kinetics

Three distinct kinetic models were employed to gain a deeper understanding of the dynamics and control of the adsorption processes, and the time-dependent data acquired for the adsorption of pomegranate peel, BBR, and VBR dyes were utilized. A plot of  $\ln(q_e - q_t)$  versus  $t$  was plotted using the pseudo-first-order kinetic model given in Eq. (3). K<sub>s1</sub> and q<sub>e</sub> values were found from the slope and intercept of the graph, respectively. A plot of  $t$  versus  $t/q_t$  was plotted using the pseudo-second-order kinetic model given in Eq. (4). q<sub>e</sub> and K<sub>s2</sub> values were found from the slope and intercept of the graph, respectively. A plot of  $t^{0.5}$  versus  $q_t$  was plotted using the intraparticle diffusion model given in Eq. 5. K<sub>p</sub> and C values were found from the slope and intercept of the graph, respectively. According to the values obtained, the equation constants, R<sup>2</sup>, χ<sup>2</sup>, HYBRID, and EABS values are presented in Table 3.

According to Table 3, the pseudo-second-order kinetic model's correlation coefficients (R<sup>2</sup>) are 0.9998 for BBR and 0.9999 for VBR. When the theoretical and experimental q<sub>e</sub> values were compared, respectively, 4.270 (mg/g) and 4.228 (± 0.05745) (mg/g) for BBR, 3.744 (mg/g) and 3.728 (± 0.001178) (mg/g) for VBR were found. Given that the R<sup>2</sup> values for both dyes are close to 1, the q<sub>e</sub> values discovered both theoretically and experimentally are also close to one another, and the error values of χ<sup>2</sup>, HYBRID and EABS are also very low. Therefore, it can be concluded that the adsorption of both dyes with pomegranate peel obeys the pseudo-second-order kinetic model. The graph of the pseudo-second-order kinetic model is given in Fig. 6.

### Adsorption isotherm

The adsorption isotherms examine the equilibrium conditions of adsorbents on an adsorbent surface. BBR and VBR adsorption data with pomegranate peel were evaluated at 4 °C, 25 °C, and 45 °C using the Freundlich, Langmuir, and D-R isotherm models. A plot of  $\ln q_e$  versus  $\ln C_e$  was plotted using the Freundlich isotherm model given in Eq. (6).  $n$  and K<sub>F</sub> values were found from the slope and intercept of the graph, respectively. A plot of  $C_e^{-1}$  versus  $q_e^{-1}$  was plotted using the Langmuir isotherm model given in Eq. (7). K<sub>L</sub> and q<sub>max</sub> values were found from the slope and intercept of the graph, respectively. A plot of  $\epsilon^2$  versus  $\ln q_e$  was plotted using the D-R isotherm model given in Eq. 8. β and  $\ln q_{\max}$  values were found from the slope and intercept of the graph, respectively. According to the values obtained, the equation constants, R<sup>2</sup>, χ<sup>2</sup>, HYBRID, and EABS values are presented in Table 4.

According to the obtained isotherm data, the Langmuir model showed the highest fit values for both BBR and VBR dyes at all three temperatures. The coefficient

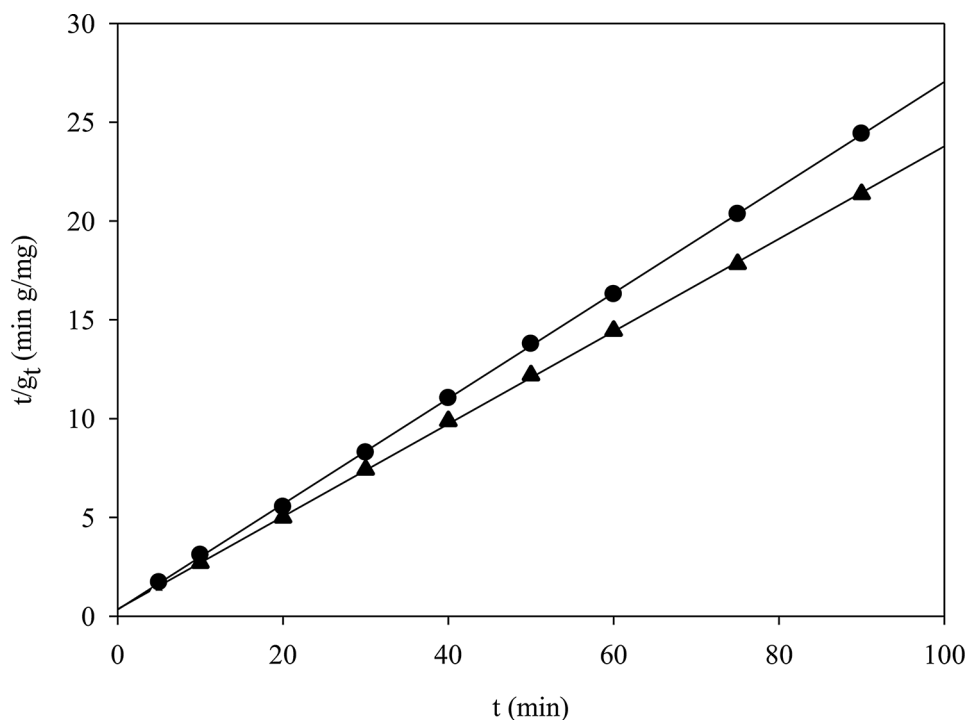


**Fig. 6** Pseudo-second-order kinetic plot of BBR (▲) and VBR (●) for adsorption with pomegranate peel (Conditions: For BBR, dye concentration=25 ppm; adsorbent amount=0.08 g; pH=2; T=25 °C±1 °C; contact time: 20 min. For VBR, dye concentration=25 mg/L; adsorbent amount=0.15 g; pH=original pH; T=25 °C±1 °C; contact time: 20 min)

**Table 4** Isotherm constants for adsorption of BBR and VBR with pomegranate Ppeel at different temperatures

Dye	T (°C)	Freundlich isotherm model					
		R <sup>2</sup>	χ <sup>2</sup>	HYBRID	EABS	K <sub>F</sub> (L/g)	n
BBR	4 °C	0.4130	1.940 10 <sup>-5</sup>	3.920 10 <sup>-5</sup>	3.010 10 <sup>-5</sup>	3.140 10 <sup>-4</sup>	3.805
	25 °C	0.6291	6.030 10 <sup>-6</sup>	7.500 10 <sup>-6</sup>	1.530 10 <sup>-5</sup>	1.150 10 <sup>-4</sup>	5.958
	45 °C	0.7716	3.990 10 <sup>-6</sup>	5.580 10 <sup>-6</sup>	1.620 10 <sup>-5</sup>	3.300 10 <sup>-4</sup>	3.747
VBR	4 °C	0.6853	9.520 10 <sup>-5</sup>	7.700 10 <sup>-5</sup>	1.460 10 <sup>-4</sup>	2.047 10 <sup>-2</sup>	1.660
	25 °C	0.8849	2.640 10 <sup>-5</sup>	3.270 10 <sup>-5</sup>	8.260 10 <sup>-5</sup>	1.188 10 <sup>-1</sup>	1.287
	45 °C	0.7406	7.150 10 <sup>-5</sup>	5.910 10 <sup>-5</sup>	1.130 10 <sup>-4</sup>	2.2778	0.9908
Dye	T (°C)	Langmuir isotherm model					
		R <sup>2</sup>	χ <sup>2</sup>	HYBRID	EABS	K <sub>L</sub> (L/mol)	q <sub>max</sub> (mol/g)
BBR	4 °C	0.9548	2.420 10 <sup>-5</sup>	4.510 10 <sup>-5</sup>	3.630 10 <sup>-5</sup>	1.501 10 <sup>5</sup>	3.070 10 <sup>-5</sup>
	25 °C	0.9255	2.880 10 <sup>-6</sup>	3.310 10 <sup>-6</sup>	1.100 10 <sup>-5</sup>	3.367 10 <sup>5</sup>	2.470 10 <sup>-5</sup>
	45 °C	0.9175	1.560 10 <sup>-6</sup>	1.950 10 <sup>-6</sup>	8.440 10 <sup>-6</sup>	6.685 10 <sup>4</sup>	3.450 10 <sup>-5</sup>
VBR	4 °C	0.9536	8.930 10 <sup>-5</sup>	7.200 10 <sup>-5</sup>	1.460 10 <sup>-4</sup>	2.090 10 <sup>4</sup>	1.040 10 <sup>-4</sup>
	25 °C	0.9577	2.590 10 <sup>-5</sup>	3.290 10 <sup>-5</sup>	7.810 10 <sup>-5</sup>	4.858 10 <sup>3</sup>	2.820 10 <sup>-4</sup>
	45 °C	0.9440	7.140 10 <sup>-5</sup>	5.990 10 <sup>-5</sup>	1.150 10 <sup>-4</sup>	6.581 10 <sup>2</sup>	3.197 10 <sup>-3</sup>
Dye	T (°C)	D-R isotherm model					
		R <sup>2</sup>	χ <sup>2</sup>	HYBRID	EABS	q <sub>max</sub> (mol/g)	β (mol <sup>2</sup> /kJ <sup>2</sup> )
BBR	4 °C	0.8149	1.990 10 <sup>-5</sup>	4.000 10 <sup>-5</sup>	3.110 10 <sup>-5</sup>	8.000 10 <sup>-5</sup>	2.320 10 <sup>-9</sup>
	25 °C	0.6619	5.660 10 <sup>-6</sup>	6.880 10 <sup>-6</sup>	1.470 10 <sup>-5</sup>	4.760 10 <sup>-4</sup>	1.280 10 <sup>-9</sup>
	45 °C	0.8001	3.540 10 <sup>-6</sup>	4.840 10 <sup>-6</sup>	1.500 10 <sup>-5</sup>	9.030 10 <sup>-5</sup>	1.940 10 <sup>-9</sup>
VBR	4 °C	0.9361	9.350 10 <sup>-5</sup>	7.440 10 <sup>-5</sup>	1.450 10 <sup>-4</sup>	9.560 10 <sup>-4</sup>	5.560 10 <sup>-9</sup>
	25 °C	0.8820	2.640 10 <sup>-5</sup>	3.270 10 <sup>-5</sup>	7.930 10 <sup>-5</sup>	2.637 10 <sup>-3</sup>	6.430 10 <sup>-9</sup>
	45 °C	0.7423	7.060 10 <sup>-5</sup>	5.850 10 <sup>-5</sup>	1.130 10 <sup>-4</sup>	1.068 10 <sup>-2</sup>	6.780 10 <sup>-9</sup>

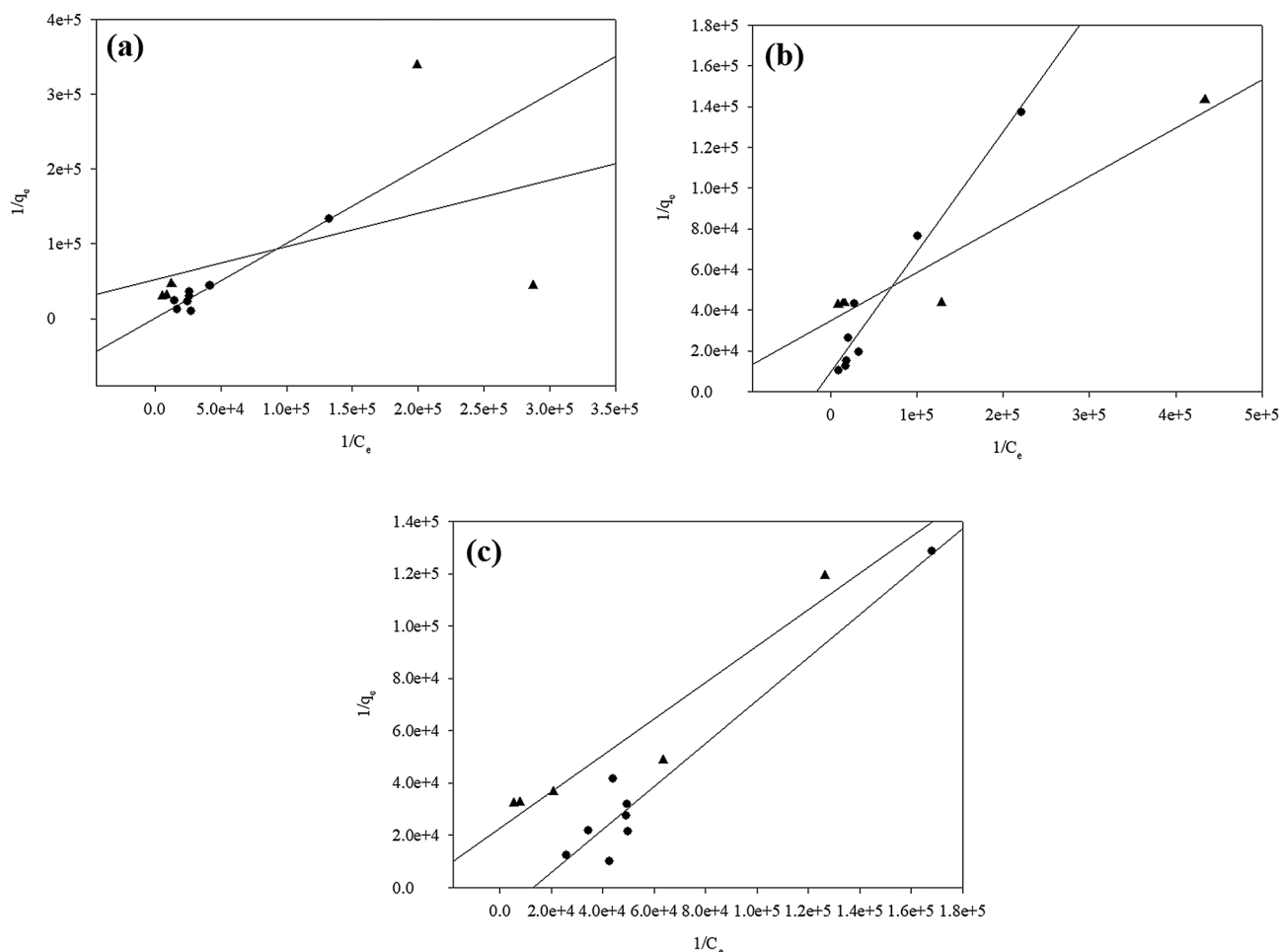


**Fig. 7** Langmuir isotherm graph of the adsorption of BBR(▲) and VBR (●) with pomegranate peel (a)  $T=4\text{ }^{\circ}\text{C}$ , (b)  $T=25\text{ }^{\circ}\text{C}$ , (c)  $T=45\text{ }^{\circ}\text{C}$  (Conditions: for BBR, dye concentration = 25 ppm; adsorbent amount = 0.08 g; pH = 2;  $T=4, 25, 45\text{ }^{\circ}\text{C}$ ; contact time: 20 min. For VBR, dye concentration = 25 mg/L; adsorbent amount = 0.15 g; pH = original pH; contact time: 20 min)

**Table 5** Thermodynamic parameters for BBR and VBR adsorption by pomegranate peel

Dye	T ( $^{\circ}\text{C}$ )	$\Delta H^{\circ}$ (kJ/mol)	$\Delta S^{\circ}$ (kJ/mol K)	$\Delta G^{\circ}$ (kJ/mol)
BBR	4 $^{\circ}\text{C}$	$-1.308 \cdot 10^4$	55.02	$-2.833 \cdot 10^4$
	25 $^{\circ}\text{C}$	$-1.308 \cdot 10^4$	55.02	$-2.949 \cdot 10^4$
	45 $^{\circ}\text{C}$	$-1.308 \cdot 10^4$	55.02	$-3.059 \cdot 10^4$
VBR	4 $^{\circ}\text{C}$	$-6.135 \cdot 10^4$	-137.6	$-2.322 \cdot 10^4$
	25 $^{\circ}\text{C}$	$-6.135 \cdot 10^4$	-137.6	$-2.033 \cdot 10^4$
	45 $^{\circ}\text{C}$	$-6.135 \cdot 10^4$	-137.6	$-1.758 \cdot 10^4$

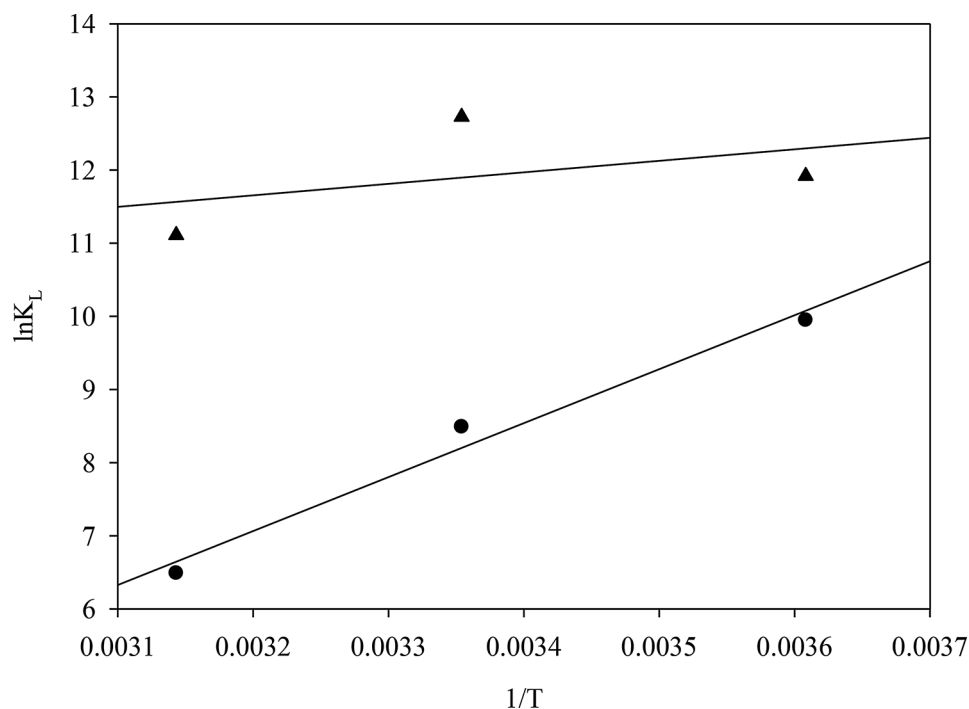
of determination ( $R^2$ ) of the Langmuir model for the BBR dye was obtained as 0.9548 at 4  $^{\circ}\text{C}$ , 0.9255 at 25  $^{\circ}\text{C}$ , and 0.9175 at 45  $^{\circ}\text{C}$ , respectively. The  $R^2$  values for the VBR dye were 0.9536 at 4  $^{\circ}\text{C}$ , 0.9577 at 25  $^{\circ}\text{C}$ , and 0.9440 at 45  $^{\circ}\text{C}$ , showing a very high correlation. In addition, the error parameters  $\chi^2$ , HYBRID, and EABS of the Langmuir model were found to be lower compared to the other isotherm models. This reveals that monolayer and homogeneous surface adsorption is the most suitable model for all temperatures examined and for both dye types.

Figure 7 shows the Langmuir isotherm graphs at 4, 25, and 45  $^{\circ}\text{C}$  for both dyes.

#### Adsorption thermodynamics

The thermodynamic parameters of adsorption of BBR and VBR with pomegranate peel were evaluated by analyzing  $\Delta G^{\circ}$ ,  $\Delta H^{\circ}$ , and  $\Delta S^{\circ}$ .  $K_L$  was used as the equilibrium constant.  $1/T$  was plotted against  $\ln K_L$ . Thermodynamic data, calculated using the slope and intercept of the graph, are presented in Table 5.

According to the data in Table 5, since the  $\Delta H^{\circ}$  obtained for both dyes is negative, the adsorption of BBR and VBR with pomegranate peel was exothermic. The negative  $\Delta G^{\circ}$  values obtained indicate that the adsorption of both dyes was a spontaneous process [48]. The  $\Delta S^{\circ}$  obtained for BBR was positive. This means that the disorder of the system increases, i.e., the entropy increases with the dispersion of dyes on the surface during adsorption [48]. The  $\Delta S^{\circ}$  obtained for VBR was negative. Entropy decreases, indicating that the dye forms a more regular



**Fig. 8** Langmuir isotherm graph of the adsorption of BBR(▲) and VBR (●) with pomegranate peel

structure during adsorption and settles on the adsorbent surface in a more organized manner [49]. (Fig. 8)

#### Adsorption mechanism

According to FT-IR analyses, the shifts observed in the characteristic peaks (especially in O–H, C=O, and CH<sub>2</sub>–O groups) after adsorption indicate that the functional groups on the pomegranate peel surface actively interact with the dye molecules. The interaction of hydroxyl and carbonyl groups with the dyes, in particular, suggests that covalent bonding may also be possible, in addition to hydrogen bonding. SEM images reveal the

change in surface morphology of the pomegranate peel after adsorption, confirming that the dyes are successfully bound to the surface. XRD analyses reveal an increase in crystallinity after adsorption, indicating the formation of a more regular surface structure. Additionally, zeta potential analyses reveal a change in surface charges before and after adsorption, indicating an electrostatic attraction between the negatively charged surface of the pomegranate peel and the cationic VBR dye. In contrast, for BBR, attraction or repulsion forces may play a role depending on the pH conditions. Kinetic studies indicate that both dyes follow the pseudo-second-order

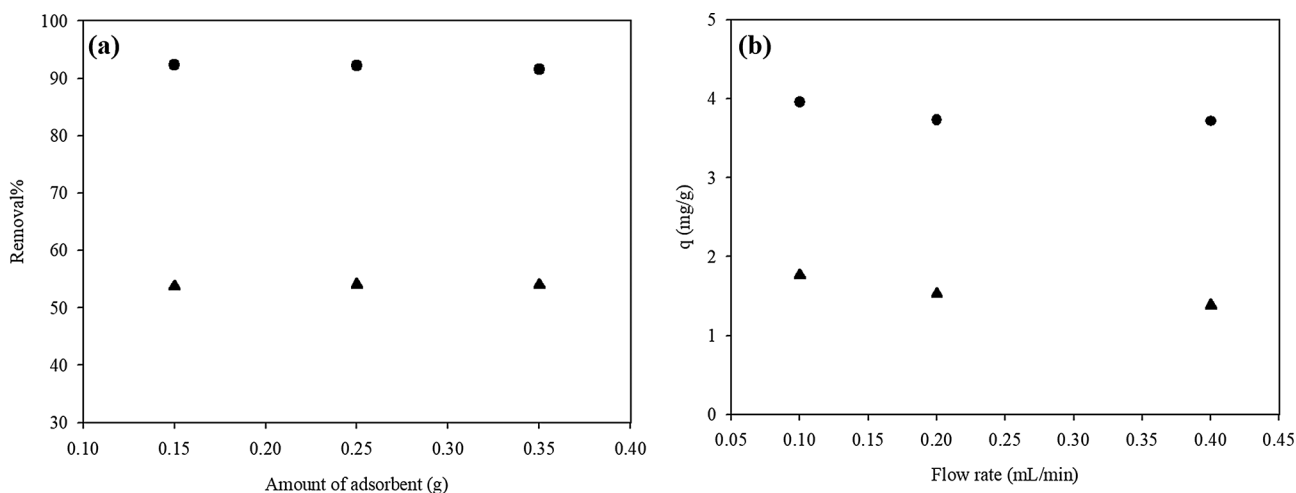


**Fig. 9** Effect of adsorbent amount (a) and flow rate (b) on the adsorption of BBR (▲) and VBR (●) with pomegranate peel in a continuous system

**Table 6** Comparison of pomegranate Peel and other adsorbents in BBR and VBR removal

Dye	Adsorbent	Experimental conditions	Removal%	Ref
BBR	nigella sativa	$C_0 = 25$ mg/L; $V = 50$ mL; $m = 0.5$ g; $t = 60$ min	$\approx 70\%$	[1]
BBR	porous nanocrystalline cobalt ferrite	$C_0 = 25$ – $200$ mg/L $pH = 1.79$ $m = 0.1$ g	93%	[11]
BBR	$\alpha$ -chitin nanoparticles	$C_0 = 5$ – $50$ mg/L $pH = 10$ $t = 25$ min	91%	[12]
BBR	wheat bran	$C_0 = 10$ mg/L $pH = 2$ $m = 0.1$ g $t = 30$ min	95.70%	[14]
BBR	apricot stone	$C_0 = 20$ mg/L $pH = 2$	39.55%	[15]
BBR	pomegranate peel	$C_0 = 25$ mg/L $V = 25$ mL $m = 0.08$ g $pH = 2$ $t = 20$ min	90.38%	This work
VBR	calcined eggshell	$C_0 = 50$ mg/L $pH = 5.62$ $m = 2.0$ g/L $t = 5$ min	97%	[17]
VBR	bone meal and chitosan biocomposite	$C_0 = 3.00$ g/L $V = 50$ mL $m = 3.00$ g/L $pH = 6$ $t = 15$ min	98.69%	[18]
VBR	pomegranate peel	$C_0 = 25$ mg/L $V = 25$ mL $m = 0.15$ g $pH =$ original pH $t = 20$ min	100%	This work

kinetic model, suggesting that adsorption occurs through chemical interactions (chemisorption). The high correlation coefficients ( $R^2 > 0.999$ ) and low error parameters ( $\chi^2$ , HYBRID, and EABS) obtained support this mechanism. In addition, the Langmuir isotherm model, which shows the best fit at all temperatures, indicates that adsorption occurs as a monolayer on a homogeneous surface. When all these findings are evaluated together, it can be concluded that the adsorption of BBR and VBR dyes onto pomegranate peel occurs primarily through chemical adsorption (chemisorption), a process supported by electrostatic attraction, functional group interactions, and  $\pi$ – $\pi$  interactions of aromatic structures [50].

#### Determination of the most suitable conditions for adsorption in the continuous system

The study investigated the effect of adsorbent quantity and flow rate on the adsorption of pomegranate peel onto BBR and VBR in a continuous system.

#### Amount of adsorbent

2 mL ejectors were selected for the column system to study the adsorption effectiveness of BBR and VBR. A flow rate of 0.1 mL/min was used to pass the BBR and VBR solutions through the column. UV spectrophotometry was used to determine the concentration of BBR and VBR in the solution exiting the column. Figure 9(a) shows the effect of the adsorbent amount on the adsorption of BBR and VBR using pomegranate peel in a continuous system. The amount of adsorbent for both dyestuffs was found to be 0.15 g. The removal percentage remained constant as the amount of adsorbent increased.

#### Effect of flow rate

The dye solutions were run through the column at varying rates, ranging from 0.1 to 0.4 mL/min, to test the impact of flow rate in a continuous system. Figure 9(b) illustrates the impact of flow rate on the adsorption of BBR and VBR using pomegranate peel in a continuous system. Despite a slight reduction, the adsorption

capacity remained relatively unchanged as the flow rate increased.

### Wastewater applications

Utilizing natural wastewater is crucial in demonstrating the study's suitability for natural environmental conditions and illustrating how adsorption can be applied in industrial settings. For this purpose, adsorption studies were conducted in the factory's natural wastewater environment under the optimal conditions of the batch system. 25 mg/L of BBR and VBR were added to the sample from the textile factory effluent. Optimum adsorption conditions (for BBR: pH 2, 0.08 g of adsorbent, and 20 min contact time; for VBR: 0.15 g of adsorbent at the original pH and 20 min contact time) were investigated. 90.38% of BBR and 100% of VBR were removed from wastewater.

Table 6. compares the dye removal performance of pomegranate peel with the removal results of BBR and VBR with different adsorbents. Pomegranate peel is a very effective adsorbent with a removal efficiency of 90.38% for BBR. Pomegranate peel, when compared to other adsorbents, showed a performance close to  $\alpha$ -chitin nanoparticles [12], although not as much as cobalt ferrite [11] and wheat bran [14]. However, it produced much more successful results than *nigella sativa* [1] and apricot stone [15]. Higher removal can be achieved by modifying the pomegranate peel to remove BBR. Pomegranate peel was the most effective adsorbent for VBR, providing 100% removal. Pomegranate peel provided the maximum removal for VBR dye, although other adsorbents, such as calcined eggshell [17] and bone meal-chitosan biocomposite [18], also had very high removal percentages.

### Conclusion

In this study, the removal of BBR and VBR dyes from aqueous solutions using pomegranate peel was investigated. Characterization studies (XRD, SEM, BET, FT-IR, TGA and zeta potential analyses) showed that pomegranate peel has high adsorption capacity in terms of surface morphology, surface area, and functional groups. In kinetic analyses, it was observed that the pseudo-second-order kinetic model provided the best fit for both dyes. This shows that chemical adsorption is the dominant mechanism. Adsorption processes were conducted at various temperatures, and the results were evaluated using three different isotherm models. The obtained data showed that the Langmuir isotherm model was the most suitable model for both dyes at all temperatures ( $R^2 > 0.91$ ). According to the Langmuir model, the maximum adsorption capacities were found to be  $6.685 \times 10^{-4}$  mol/g for BBR and  $3.197 \times 10^{-3}$  mol/g for VBR. When thermodynamic parameters were examined, it was determined that adsorption was an exothermic

and spontaneous process for both dyes. For BBR adsorption,  $\Delta H^\circ$  -1.308 kJ/mol and  $\Delta G^\circ$   $-3.059 \times 10^4$  kJ/mol were obtained; for VBR adsorption,  $\Delta H^\circ$  -6.135 kJ/mol and  $\Delta G^\circ$   $-1.758 \times 10^4$  kJ/mol were found. As a result, pomegranate peel was evaluated as a low-cost, environmentally friendly, and effective adsorbent, demonstrating that it offers a sustainable alternative for removing textile dyes. The used adsorbent can be disposed of through controlled incineration, minimizing environmental impacts, or utilized as a filling material in the construction sector. In this way, it can contribute to environmental sustainability in terms of waste management.

### Author contributions

B.A. did the experimental part, did the calculations, and wrote this article.

### Funding

Not applicable.

### Data availability

No datasets were generated or analysed during the current study.

### Declarations

#### Ethics approval and consent to participate

Ethical approval - not applicable for both human and animal studies.

#### Consent for publication

Not applicable.

#### Competing interests

The authors declare no competing interests.

Received: 9 December 2024 / Accepted: 4 April 2025

Published online: 16 April 2025

### References

1. Abdel-Ghani NT, El-Chaghaby GA, Rawash ES, Lima EC. Adsorption of coomassie brilliant blue R-250 dye onto novel activated carbon prepared from *Nigella sativa* L. waste: equilibrium, kinetics and thermodynamics. *J Chil Chem Soc.* 2017. <https://doi.org/10.4067/S0717-97072017000200016>.
2. Zhu M-X, Li Y-P, Xie M, Xin H-Z. Sorption of an anionic dye by uncalcined and calcined layered double hydroxides: a case study. *J Hazard Mater.* 2005. <https://doi.org/10.1016/j.jhazmat.2004.12.029>.
3. Thamer BM, Aldalbahi A, Moydeen M, El-Hamshary H, Al-Enizi AM, El-Newehy MH. Effective adsorption of coomassie brilliant blue dye using poly(phenylene diamine)grafted electrospun carbon nanofibers as a novel adsorbent. *Mater Chem Phys.* 2019. <https://doi.org/10.1016/j.matchemphys.2019.05.087>.
4. Chen CY, Tsai TH, Wu PS, Tsao SE, Huang YS, Chung YC. Selection of electrogenic bacteria for microbial fuel cell in removing Victoria blue R from wastewater. *J Environ Sci Health Part A.* 2017. <https://doi.org/10.1080/10934529.2017.1377580>.
5. Lee J-R, Jalani JC, Arshad ZIM, dos Santos JCS, Mudalip SKA, Shaarani SM, Sulaiman SZ. Optimization of Victoria blue R dye biodegradation by pineapple waste garbage enzymes. *J Adv Res Appl Sci Eng Tech.* 2024. <https://doi.org/10.37934/araset.35.2.110>.
6. Oladipo AA, Gazi M. Enhanced removal of crystal Violet by low cost alginate/acid activated bentonite composite beads: optimization and modelling using non-linear regression technique. *J Water Process Eng.* 2014. <https://doi.org/10.1016/j.jwpe.2014.04.007>.
7. Tzvetkov G, Kaneva N, Spassov T. Room-temperature fabrication of core-shell nano-ZnO/pollen grain biocomposite for adsorptive removal of organic dye from water. *Appl Surf Sci.* 2017. <https://doi.org/10.1016/j.apsusc.2016.12.225>.

8. Karimi K, Fatemi S. Methane capture and nitrogen purification from a nitrogen rich reservoir by pressure swing adsorption; experimental and simulation study. *J Environ Chem Eng*. 2021. <https://doi.org/10.1016/j.jece.2021.106210>.
9. Vijayaraghavan K, Yun YS. Bacterial biosorbents and biosorption. *Biotechnol. Adv*. 2008. <https://doi.org/10.1016/j.biotechadv.2008.02.002>.
10. Volesky B. Sorption and biosorption. Montreal: BV Sorbex, Inc.; 2003.
11. Khan MA, Alam MM, Naushad M, Allothman ZA, Kumar M, Ahamad T. Sol-gel assisted synthesis of porous nano-crystalline  $\text{CoFe}_2\text{O}_4$  composite and its application in the removal of brilliant blue-R from aqueous phase: an eco-friendly and economical approach. *Chem Eng J*. 2015. <https://doi.org/10.1016/j.cej.2015.05.042>.
12. Dhananasekaran S, Palanivel R, Pappu S. Adsorption of methylene blue, bromophenol blue, and coomassie brilliant blue by  $\alpha$ -chitin nanoparticles. *J Adv Res*. 2016. <https://doi.org/10.1016/j.jare.2015.03.003>.
13. Bangash FK, Alam S. Brilliant blue R adsorption from aqueous solution on activated carbon produced from corncob waste. *J Chin Chem Soc*. 2007. <http://doi.org/10.1002/jccs.200700086>.
14. Ata S, Din MI, Rasool A, Qasim I, Mohsin IU. Equilibrium, thermodynamics, and kinetic sorption studies for the removal of coomassie brilliant blue on wheat Bran as a low-cost adsorbent. *J Anal Methods Chem*. 2012. <https://doi.org/10.1155/2012/405980>.
15. Abbas M, Cherfi A, Kaddour S, Aksil T. Adsorption in simple batch experiments of coomassie blue G-250 by apricot stone activated carbon-Kinetics and isotherms modelling. *Desalin Water Treat*. 2016. <https://doi.org/10.1080/19443994.2015.1067871>.
16. Prasad RN, Viswanathan S, Devi JR, Rajkumar J, Parthasarathy N. Kinetics and equilibrium studies on biosorption of CBB by Coir pith. *Am -Eurasian J Sci Res*. 2008. 123–7.
17. Tosun-Satir I, Erol K. Calcined eggshell for removal of Victoria blue R dye from wastewater medium by adsorption. *J Turkish Chem Soc Sect Chem*. 2021;47–56. <https://doi.org/10.18596/jotcsa.760083>.
18. Tosun Satir I, Ozdemir N, Donmez Gungunes C. Bone meal and Chitosan biocomposite: a new biosorbent for the removal of Victoria blue R from wastewater. *Chem Eng Commun*. 2022. <https://doi.org/10.1080/00986445.2021.1957850>.
19. Erol K, Köse K, Köse DA, Sızır U, Tosun Satir I, Uzun L. Adsorption of Victoria blue R (VBR) dye on magnetic microparticles containing Fe(II)–Co(II) double salt. *Desalin Water Treat*. 2016. <https://doi.org/10.1080/19443994.2015.1030708>.
20. Sanchez-Martin J, Beltran-Heredia J, Gragera-Carvajal J. *Caesalpinia spinosa* and *castanea sativa* tannins: A new source of biopolymers with adsorbent capacity. Preliminary assessment on cationic dye removal. *Ind Crops Prod*. 2011. <https://doi.org/10.1016/j.indcrop.2011.03.024>.
21. Oladipo AA, Gazi M. Two-stage batch Sorber design and optimization of biosorption conditions by Taguchi methodology for the removal of acid red 25 onto magnetic biomass. *Korean J Chem Eng*. 2015. <https://doi.org/10.1007/s11814-015-0001-6>.
22. Kaderides K, Kyriakoudi A, Mourtzinos I, Goula AM. Potential of pomegranate Peel extract as a natural additive in foods. *Trends Food Sci Technol*. 2021. <http://doi.org/10.1016/j.tifs.2021.06.050>.
23. Moradi AG, Rahmani F, Aziz AS, Qiami MF. Effects of feeding pomegranate Peel silage on feed intake and growth performance of Turkey bred sheep. *Int J Agril Res Innov Tech*. 2020. <https://doi.org/10.3329/ijariv.v10i2.51588>.
24. Bhatnagar A, Minocha AK. Adsorptive removal of 2,4-dichlorophenol from water utilizing *Punica granatum* Peel waste and stabilization with cement. *J Hazard Mater*. 2009. <https://doi.org/10.1016/j.jhazmat.2009.02.151>.
25. Sahin A, Gül UD, Bayazit G, Kaynak MS. Thermosensitive gel of pomegranate Peel extract as alternative for the treatment of local infections. *Acta Pharm Sci*. 2024. <https://doi.org/10.23893/1307-2080.APS6241>.
26. Waghmare C, Ghodmare S, Ansari K, Alfaisal FM, Alam S, Khan MA, Ezaier Y. Adsorption of methylene blue dye onto phosphoric acid-treated pomegranate Peel adsorbent: kinetic and thermodynamic studies. *Desalin Water Treat*. 2024. <https://doi.org/10.1016/j.dwt.2024.100406>.
27. Afshin S, Poureshgh Y, Rashtbari Y, Fazlzadeh M, Asl FB, Hamzezhadeh A, Pormazari SM. Eco-friendly cost-effective approach for synthesis of ZnO nanoparticles and loaded on worn tire powdered activated carbon as a novel adsorbent to remove organic dyes from aqueous solutions: equilibrium, kinetic, regeneration and thermodynamic study. *Desalin Water Treat*. 2021. <https://doi.org/10.5004/dwt.2021.27283>.
28. Rashtbari Y, Arfaeina H, Ahmadi S, Asl FB, Afshin S, Poureshgh Y, Fazlzadeh M. Potential of using green adsorbent of humic acid removal from aqueous solutions: equilibrium, kinetics, thermodynamic and regeneration studies. *J Environ Anal Chem*. 2020. <https://doi.org/10.1080/03067319.2020.1796993>.
29. Lagergren S, Lagergren S, Lagergren SY, Sven K. Zur theorie der sogenannten adsorption gelöster Stoffe. *Zeitschr F Chem Und Ind Der Kolloide*. 1907. <https://doi.org/10.1007/BF01501332>.
30. Ho Y, McKay G. Kinetic models for the sorption of dye from aqueous solution by wood. *Process Saf Environ Prot*. 1998. <https://doi.org/10.1205/09575829829326>.
31. Weber WJ, Morris JC. Kinetics of adsorption on carbon from solution. *J Sanit Eng Div*. 1963. <https://doi.org/10.1061/JSEDAI.0000430>.
32. Freundlich H. Über die adsorption in lösungen. *Z f f r Phys Chem*. 1907;57:385–470.
33. Langmuir I. The adsorption of gases on plane surfaces of glass, mica and platinum. *J Am Chem Soc*. 1918. <https://doi.org/10.1021/ja02242a004>.
34. Dubinin MM, Radushkevich LV. The equation of the characteristic curve of the activated charcoal. *USSR Phys Chem Sect*. 1947;55:331–33.
35. Ansari H, Oladipo AA, Gazi M. Alginate-based porous polyhipe for removal of single and multi-dye mixtures: competitive isotherm and molecular Docking studies. *Int J Biol Macromol*. 2023. <https://doi.org/10.1016/j.jbiomac.2023.125736>.
36. Miraboutalebi SM, Nikouzad SK, Peydayesh M, Allahgholi N, Vafajoo L, McKay G. Methylene blue adsorption via maize silk powder: kinetic, equilibrium, thermodynamic studies and residual error analysis. *Process Saf Environ Prot*. 2017. <https://doi.org/10.1016/j.psep.2017.01.010>.
37. Bulut Kocabas B, Tosun Satir I. Investigation of the Chitosan immobilized eggshell for the biosorption of brilliant blue R dye. *Hittite J Sci Eng*. 2019. <http://doi.org/10.17350/HJSE19030000159>.
38. Bilgin E, Erol K, Kose K, Kose DA. Use of nicotinamide decorated polymeric cryogels as heavy metal sweeper. *Environ Sci Pollut Res Int*. 2018. <https://doi.org/10.1007/s11356-018-2784-6>.
39. Ji W, Jin H, Wang H, Tabassum S, Lou Y, Fan X, Ren M, Wang J. Elucidating the dominant role of  $\pi$ - $\pi$  interactions in methylene blue removal via porous Biochar: A synergistic approach of experimental and theoretical mechanistic insights. *Colloids Surf A: Physicochem Eng Asp*. 2025. <https://doi.org/10.1016/j.colsurfa.2025.136615>.
40. Rout PR, Bhunia P, Dash RR. A mechanistic approach to evaluate the effectiveness of red soil as a natural adsorbent for phosphate removal from wastewater. *Desalin Water Treat*. 2015. <https://doi.org/10.1080/19443994.2014.881752>.
41. Reyes-Gasga J, Martínez-Piñeiro EL, Rodríguez-Álvarez G, Tiznado-Orozco GE, García-García R, Brès EF. XRD and FTIR crystallinity indices in sound human tooth enamel and synthetic hydroxyapatite. *Mater Sci Eng C*. 2013. <https://doi.org/10.1016/j.msec.2013.07.014>.
42. Danaei M, Dehghankhold M, Ataei S, Davarani FH, Javanmard R, Dokhani A, Khorasani S, Mozafari MR. Impact of particle size and polydispersity index on the clinical applications of lipidic nanocarrier systems. *Pharmaceutics*. 2018. <https://doi.org/10.3390/pharmaceutics10020057>.
43. Sulistyaningsih T, Sari DA, Widiarti N, Astuti W, Wulandari R, Harjunowibowo D. Green synthesis of Gaharu leaf extract-modified magnetite as an adsorbent for Methyl orange textile dyes. *Waste Manag Bull*. 2024. <https://doi.org/10.1016/j.wmb.2024.02.007>.
44. Yuan Z-Y, Su B-L. Insights into hierarchically meso-macroporous structured materials. *J Mater Chem*. 2006. <https://doi.org/10.1039/b512304f>.
45. Akafu T, Chimdi A, Gomoro K. Removal of fluoride from drinking water by sorption using diatomite modified with aluminum hydroxide. *J Anal Methods Chem*. 2019. <https://doi.org/10.1155/2019/4831926>.
46. Hashem A, Aniagor CO, Fikry M, Taha GM, Badawy SM. Characterization and adsorption of Raw pomegranate Peel powder for lead (II) ions removal. *J Mater Cycles Waste Manag*. 2023. <https://doi.org/10.1007/s10163-023-01655-2>.
47. Wang J, Zhang J, Han L, Wang J, Zhu L, Zeng H. Graphene-based materials for adsorptive removal of pollutants from water and underlying interaction mechanism. *Adv Colloid Interface Sci*. 2021. <https://doi.org/10.1016/j.cis.2021.102360>.
48. Debamita C, Rampal NI, Gautham JP, Vairavel P. Process optimization, isotherm, kinetics, and thermodynamic studies for removal of remazol brilliant Blue-R dye from contaminated water using adsorption on guava leaf powder. *Desalin Water Treat*. 2020. <https://doi.org/10.5004/dwt.2020.25395>.
49. Ouahabi IE, Slimani R, Hachoumi I, Anouar F, Taoufik N, Elmchauri A, Lazar S. Adsorption of a cationic dye (Yellow basic 28) onto the calcined mussel shells: kinetics, isotherm and thermodynamic parameters. *Mediterr J Chem*. 2015;4(5):261–70.

50. Irwan SA, Jawad AH, Deris RRR, Musa SA, Wu R, ALothman ZE. Blended mangosteen/pomegranate peels as a precursor for porous carbon material via microwave assisted–potassium carbonate activation: Box-Benken design optimization for Fuchsin basic and methylene Violet dyes removal. *Diam Relat Mater*. 2025. <https://doi.org/10.1016/j.diamond.2024.111846>.

### **Publisher's note**

Springer Nature remains neutral with regard to jurisdictional claims in published maps and institutional affiliations.